Chem. Senses 28: 705–716, 2003 DOI: 10.1093/chemse/bjg063

Whole-cell Recordings and Photolysis of Caged Compounds in Olfactory Sensory Neurons Isolated from the Mouse

Laura Lagostena and Anna Menini

International School for Advanced Studies, SISSA, Sector of Neurobiology, Via Beirut 2–4, 34014 Trieste, Italy

Correspondence to be sent to: Anna Menini, International School for Advanced Studies, SISSA, Via Beirut 2–4, 34014 Trieste, Italy. e-mail: menini@sissa.it

Abstract

Gene manipulation and molecular biological techniques for the study of olfaction are well developed in mice, while electrophysiological properties of mouse olfactory sensory neurons have been less extensively investigated. We used the whole-cell voltage-clamp technique in mouse isolated olfactory sensory neurons to investigate both voltage-gated and transduction currents. Voltage-gated currents were composed of transient inward currents followed by outward currents with transient and sustained components. Of the tested olfactory sensory neurons,12% responded to the odorant cineole with an inward current. Caged compounds were introduced into the cytoplasm through the patch pipette and flash photolysis of caged cyclic nucleotides activated an inward current in 94% of the cells. When the flash was localized at the cilia, the response latency, rising time and duration were shorter than when the flash illuminated the soma. The amplitude of the photolysis response was dependent on light intensity and the relation was fitted by the Hill equation, with a Hill coefficient of 3.2. These results demonstrate that it is possible to obtain recordings in the whole-cell configuration from olfactory sensory neurons isolated from the mouse and that voltage-gated currents and transduction properties are largely similar to those of amphibians.

Key words: cAMP, cGMP, odorant, olfaction, olfactory transduction, patch-clamp

Introduction

The olfactory system can detect the presence of low concentrations of odorant molecules and discriminate even very small differences among molecules with very similar chemical structure. The first event in olfaction is the binding of molecules to odorant receptors, expressed in the cilia of olfactory sensory neurons. The binding of odorant molecules initiates a transduction cascade that leads, via G-protein and adenylyl cyclase activation, to an increase in the concentration of cAMP, which directly gates ion channels in the cilia (for reviews, see Schild and Restrepo, 1998; Menini, 1999; Firestein, 2001; Breer, 2003). The opening of cAMP-gated channels (Nakamura and Gold, 1987) induces an inward transduction current carried by Na^+ and Ca^{2+} ions (Frings *et al.*, 1995; Gavazzo *et al.*, 2000), and the increase in intracellular Ca^{2+} concentration (Restrepo *et al.*, 1990; Leinders-Zufall *et al.*, 1997, 1998) produces the activation of a Ca^{2+}-activated Cl^- current that contributes to the depolarization of the cilia (Kleene and Gesteland, 1991; Kleene, 1993; Kurahashi and Yau, 1993; Zhainazarov and Ache, 1995; Frings *et al.*, 2000). The depolarization spreads passively to the dendrite and soma, triggering action potentials that are conducted along the axon to the olfactory bulb. A second olfactory transduction mechanism, involving the generation of inositol 1,4,5-triphosphate (IP_3), has also been proposed but its role in vertebrates is still controversial (for review, see Schild and Restrepo, 1998).

The electrophysiological properties of olfactory sensory neurons have been much studied in amphibians whereas have been studied less extensively in the mouse, mainly because amphibian cells are larger and less fragile than mouse cells, and their size is more suitable for patch-clamp recordings. However, in recent years, many molecular biological studies and the applications of gene manipulation techniques for the study of olfaction have been developed, mainly in mice (for review, see Mombaerts, 1999; Buck, 2000). To combine the results of these techniques with the functional properties of olfactory sensory neurons and to obtain a better understanding of the molecular mechanisms of olfactory transduction, it is therefore of great importance to be able to obtain electrophysiological recordings from olfactory sensory neurons isolated from the mouse.

Some elegant investigations on the odorant-induced responses of individual olfactory sensory neurons from the mouse have been carried out by using the cell-attached

patch-clamp technique (Maue and Dionne, 1987), the suction pipette technique in isolated cells (Reisert and Matthews, 2001) or the perforated patch-clamp technique in individual cells from the intact olfactory epithelium (Ma *et al.*, 1999; Ma and Shepherd, 2000), and important information on odorant-induced responses of mouse olfactory sensory neurons has been obtained by these studies. We investigated the possibility of obtaining electrophysiological recordings from isolated mouse olfactory sensory neurons in the whole-cell configuration, a technique that allows the introduction of compounds in the cell's cytoplasm. We measured voltage-gated currents, odorant-induced currents and currents induced by flash photolysis of caged cyclic nucleotide introduced into the olfactory sensory neuron's cytoplasm through the patch pipette.

Materials and methods

Dissociation of mouse olfactory sensory neurons

Four- to six-week-old BALB/c mice were anesthetized and killed, and their turbinates with the olfactory epithelia were quickly removed. We prepared isolated mouse olfactory sensory neurons both with and without the use of enzymes. For enzymatically dissociated cells, we used a protocol very similar to that described by Bozza and Kauer (1998). For mechanically dissociated cells, the phase of incubation with enzymes was omitted. The olfactory epithelium was dissected at 4°C and minced with fine forceps in low-Ca^{2+} mammalian Ringer's solution (in mM: 140 NaCl, 5 KCl, 10 HEPES, 1 EDTA, 10 glucose and 1 sodium pyruvate, pH 7.2) supplemented with 1 mM cysteine. The tissue was incubated in 1 U/ml papain for 25 min at room temperature; the reaction was terminated with 1 ml of Ringer's solution (in mM: 140 NaCl, 5 KCl, 1 $CaCl_2$, 1 $MgCl_2$, 10 HEPES, 10 glucose and 1 sodium pyruvate, pH 7.2), with 0.1 mg/ml BSA, 200 μg/ml leupeptin and 0.025 mg/ml DNase I. Cells were washed, resuspended in Ringer's solution, gently triturated with a flame-polished Pasteur pipette and plated on glass coverslips. Before use, dissociated olfactory sensory neurons were allowed to settle for 45–60 min at 4°C. Dissociated preparations were constantly perfused with normal Ringer's solution (2 ml/min). Olfactory sensory neurons were viewed with an inverted microscope (Olympus IX70) with an oil-immersion 100× objective and identified by their characteristic bipolar shape. Only olfactory sensory neurons with well detectable cilia were used for the experiments (see Figure 1). Electrophysiological investigations did not reveal any difference between mechanically and enzymatically dissociated olfactory sensory neurons (data not shown) but, since the use of enzymes produced a higher number of intact neurons, we preferred to use enzymatic dissociation.

Patch-clamp recording

Currents were measured with the Axopatch 200B patch-clamp amplifier (Axon Instruments, Union City, CA) in the whole-cell voltage-clamp mode. Patch pipettes were fabricated using borosilicate capillaries (WPI, Sarasota, FL) and pulled using a P-87 pipette puller (Sutter Instruments, Novato, CA). Pipette resistances were 5–10 MΩ when filled with the internal solution. Voltage-gated currents were low-pass filtered at 5 kHz and digitized at 10 kHz, while currents induced by odorants, IBMX or cyclic nucleotides were filtered at 1 kHz and digitized at 2 kHz by the analog-to-digital interface Digidata 1322A (Axon Instruments). Acquisition, storage and analysis of data were performed using PClamp 8.2 software (Axon Instruments). Resting membrane potential was measured as the potential at which the current was zero. Experiments were performed at room temperature.

Solutions

The extracellular mammalian Ringer solution contained (mM): 140 NaCl, 5 KCl, 1 $CaCl_2$, 1 $MgCl_2$, 10 HEPES, 10 glucose and 1 sodium pyruvate, pH 7.2. Whole-cell pipette solutions contained (mM): 145 KCl, 4 $MgCl_2$, 0.5 EGTA, 10 HEPES, 1 ATP and 0.1 GTP, pH 7.4. Chemicals, unless otherwise indicated, were purchased from Sigma. A 0.5 M stock solution of the odorant cineole was prepared in dimethylsulfoxide (DMSO) and diluted in the mammalian Ringer solution to the final concentration. 3-isobutyl-1-methyl-xanthine (IBMX) was prepared in 0.1 M stock solution in DMSO and diluted into the final concentration with Ringer solution. Stimulus delivery was accomplished by a perfusion system similar to that previously used to deliver odorants to salamander isolated olfactory sensory neurons (Firestein *et al.*, 1993; Menini *et al.*, 1995). An olfactory sensory neuron in the whole-cell configuration was positioned in front of one pipe from which Ringer solution was continuously flowing and then rapidly moved in front of an adjacent pipe, where an odorant– or IBMX–Ringer solution was flowing. Movements and exposure times were accomplished by a stepping motor under computer control.

For experiments on currents induced by intracellular cyclic nucleotides, cAMP was dissolved in the pipette solution at the indicated concentration and diffused into the cell after the membrane patch was ruptured to obtain the whole-cell configuration (Figure 6A).

The caged cyclic nucleotides *P*-[1-(2-nitrophenyl)ethyl]guanosine-3,5-cyclic monophosphate (caged cGMP) or *P*-[1-(2-nitrophenyl)ethyl]adenosine-3,5-cyclic monophosphate (caged cAMP) (Dojin, Japan) were dissolved in DMSO at 0.1 M and stored at –20°C. The final concentration of 0.5–1 mM was obtained by diluting an aliquot of the stock solution into the pipette solution.

Photolysis of caged compounds

Caged compounds, prepared as described in the previous section, were allowed to diffuse freely from the patch-pipette into the cytoplasm of an olfactory sensory neuron for at least two minutes after establishment of the whole-cell configuration. For flash photolysis of the caged compounds we used two different light sources. In a first set of experiments (Figures 6–8) we used a 100 W mercury lamp, and timing and duration of light flashes were regulated by a shutter (UniBlitz T132, Vincent Associates, Rochester, NY) controlled by a computer. In a second set of experiments (Figures 8–11), flash photolysis of caged compounds was produced by a Xenon flash-lamp system JML-C2 (Rapp OptoElectronic GmbH, Hamburg, Germany) coupled to the epifluorescence port of the microscope with a quartz light guide of variable diameter to reduce the size of the light spot.

Data analysis

The voltage-gated activation and inactivation curves (Figure 3) were fitted to the following Boltzmann equation:

$$I/I_{max} = 1/[1+\exp((V_{1/2}-V)/k)] \quad (1)$$

where I is the peak sodium current, I_{max} the maximal peak sodium current, V is the membrane potential, $V_{1/2}$ is the membrane potential at which I is half of I_{max} and k is the slope constant.

Data analysis was performed using PClamp 8.2 software. Data are given as mean ± standard error and the total number of observations (n), unless otherwise indicated.

Results

Olfactory sensory neurons were isolated from the mouse olfactory epithelium as described in the Methods section. Isolated olfactory sensory neurons had a cell body with a diameter of ~5–7 μm from which a dendrite of ~1 μm in diameter emerged. The dendrite had a variable length from just a few microns up to 30 μm. By carefully focusing with a 100× objective, it was possible to visualize and identify fine cilia sprouting off the knob of the olfactory sensory neuron dendrite. Two typical olfactory sensory neurons are shown in Figure 1.

By carefully approaching olfactory sensory neurons with a fine patch pipette, it was possible to obtain whole-cell voltage-clamp recordings. Stable electrical recordings were obtained in 237 isolated olfactory sensory neurons. The mean value for the resting potential, V_o, was –55.4 ± 3.6 mV (mean ± SD) and ranged between –90 to –45 mV. We found that 90% of the cells had V_o between –60 and –45 mV, with a mean of –53 ± 0.9 mV, and that the remaining 10 % had scattered values between –90 and –70 mV, with a mean of –77.5 ± 1.9 mV.

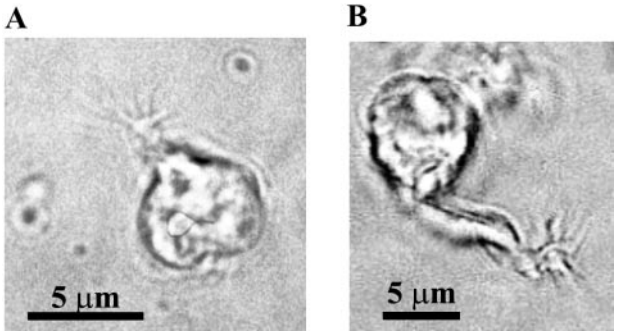

Figure 1 Photomicrographs of mouse isolated olfactory sensory neurons. Dissociated olfactory sensory neurons with short **(A)** or longer **(B)** dendrite are shown. Some cilia are visible, although near the limit of optical resolution. A 100× oil immersion objective was used. A patch-clamp pipette is out of focus in the upper-left portion of (A). The scale bar of 5 μm is the same for both photographs.

Voltage-gated currents

Representative voltage-gated currents from an isolated mouse olfactory sensory neuron are shown in Figure 2A. Depolarizing steps from a holding potential of –90 mV elicited transient inward currents followed by outward currents. The corresponding current–voltage relations measured at the peak of the inward currents or at the end of the sustained outward currents are shown in Figure 2B. The inward current is carried, almost entirely, by sodium since it was abolished by replacing external sodium with choline (data not shown). The current–voltage relationship showed that the inward current was activated between –70 and –60 mV.

Figure 2C illustrates current–voltage relationship from the same cell as in A. When the holding potential was changed to –80 or –70 mV inward currents of smaller amplitude were evoked. These current–voltage curves show that the inward current activated at different voltages depends on the holding potential, and this is likely caused by a partial inactivation of sodium channels, as shown in Figure 3.

Properties of the inward currents were further investigated by measuring activation and inactivation curves. Activation was measured by using a pre-pulse potential of –120 mV for 300 ms and then applying depolarizing voltage steps of 25 ms. Peak currents at each voltage were normalized to the maximal current and plotted as a function of voltage in Figure 3A. The relation between the normalized current and the membrane voltage was fitted by a single Boltzmann equation (see equation 1) with a half-activation voltage $V_{1/2}$ = –75.1 ± 0.4 mV and k = 5.6 ± 0.3 mV (n = 5).

To measure the inactivation properties of the sodium current, we measured the steady-state voltage-dependence of inactivation by using a two-pulse protocol. First, cells were held for 300 ms at voltages from –120 to –50 mV to achieve steady-state inactivation of sodium channels, and

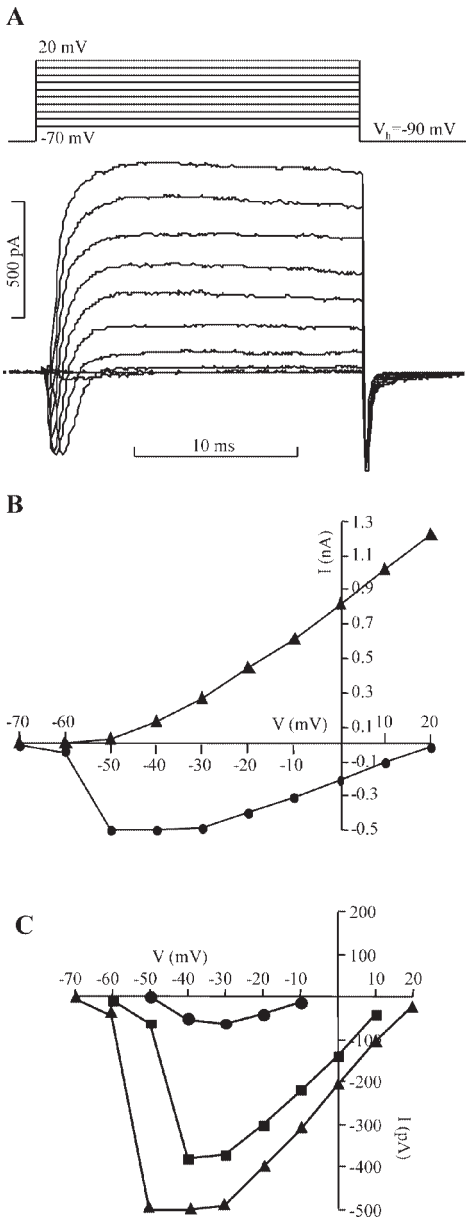

Figure 2 Whole-cell voltage-gated currents in a mouse olfactory sensory neuron. **(A)** Voltage-gated currents were elicited by 20 ms voltage steps from –70 to +20 mV from a holding potential of –90 mV, according to the voltage protocol shown in the upper trace. **(B)** Current–voltage relations from the recordings in (A) for the peak inward current (circles) or the sustained current at the end of the pulse (triangles). **(C)** Current–voltage relations for the peak inward currents elicited in the same cell shown in (A) at various holding potentials: –90 mV (triangles), –80 mV (squares), –70 mV (circles).

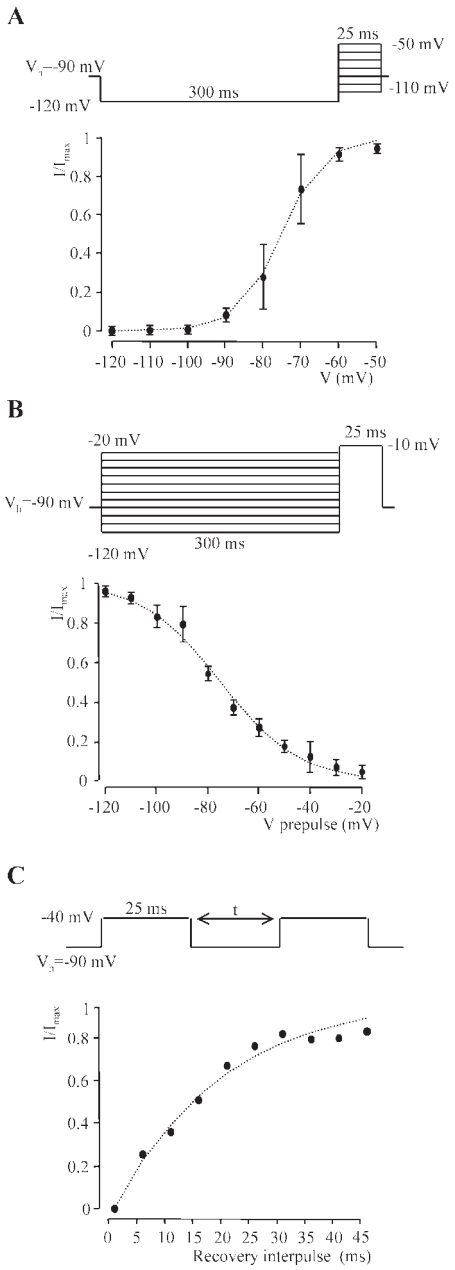

Figure 3 Activation and inactivation properties of Na+ currents in mouse olfactory sensory neurons. **(A)** Activation curve. Currents were evoked by the voltage protocol shown in the upper trace: a 300 ms prepulse at –120 mV was followed by 25 ms test pulses from –110 to –50 mV. The peak inward current at each test pulse was normalized to the maximal current and plotted versus the voltage. Mean values (± SEM) from five cells. Dotted line is the fit to a Boltzmann equation with $V_{1/2}$ = –75.1 ± 0.4 mV and k = 5.6 ± 0.3 mV. **(B)** Steady-state inactivation curve. Currents were elicited by the voltage protocol shown in the upper trace: a 300 ms prepulse to the various indicated voltages was followed by a test pulse to –10 mV. The peak inward current elicited by the test pulse was normalized to the maximal value and plotted versus the prepulse voltage. Mean values (± SEM) from four cells. Dotted line is the fit to a Boltzmann equation with $V_{1/2}$ = –75.0 ± 1.0 mV and k = –15.1 ± 0.9 mV. **(C)** Recovery from inactivation. Using a paired-pulse protocol as illustrated in the upper trace, the current elicited by the second pulse was measured and normalized to the current obtained from the first pulse and plotted versus the interpulse interval. Dotted line is the fit to a single exponential equation $I/I_{max} = 1 - e^{-t/\tau}$ with τ = 20 ms.

then a test pulse to –40 mV was given to elicit the residual current that had not been inactivated. Currents were normalized to the maximal value and plotted as a function of the pre-pulse voltage in Figure 3B. The best fit of the Boltzmann equation to the data gave $V_{1/2}$ = –75.0 ± 1.0 mV and k = –15.1 ± 0.9 mV (n = 4). The rate of recovery from inactivation was studied by using a paired-pulse protocol. A

pair of 25 ms identical pulses to –40 mV separated by a variable time, t, were applied to the cell from a holding potential of –90 mV. As the interval between pulses increased, channels recovered from inactivation and the amplitude of the sodium current induced by the second pulse gradually recovered towards the control size. The ratio of the peak current evoked by the second pulse to that evoked by the first pulse was plotted as a function of the time interval between the two pulses in Figure 3C. The recovery was described by the exponential function

$$I/I_{max} = (1 - e^{-t/\tau})$$

where τ is the recovery time constant for sodium inactivation. The best fit to the data gave $\tau = 20 \pm 1$ ms ($n = 2$).

Outward currents in response to step depolarizations of 50 ms duration from a holding potential of –50 mV are shown in Figure 4A. The outward currents were characterized by a transient and a sustained component. The lower trace in Figure 4A shows that bath application of 20 mM TEA, a well known blocker of K^+ channels, strongly reduced the two components suggesting that they are due to opening of voltage-gated K^+ channels. Current–voltage curves for the family of traces in Figure 4A were measured at the peak of the current or at the end of the sustained outward current and plotted in B. These results are consistent with the presence of two K^+ current components: a rapidly inactivating, I_A, and a delayed rectifier, I_K, component. In some olfactory sensory neurons only a delayed rectifier current appeared to be present at a holding potential of –50 mV, as illustrated in Figure 4C. If these cells were hyperpolarized to –80 mV and then depolarized, the I_A current was also elicited. All together we found that from a total of 237 cells, both I_K and I_A were present. However in 66% cells I_A could already be activated by depolarization from a holding potential of –50 mV, while in the remaining 34% cells a

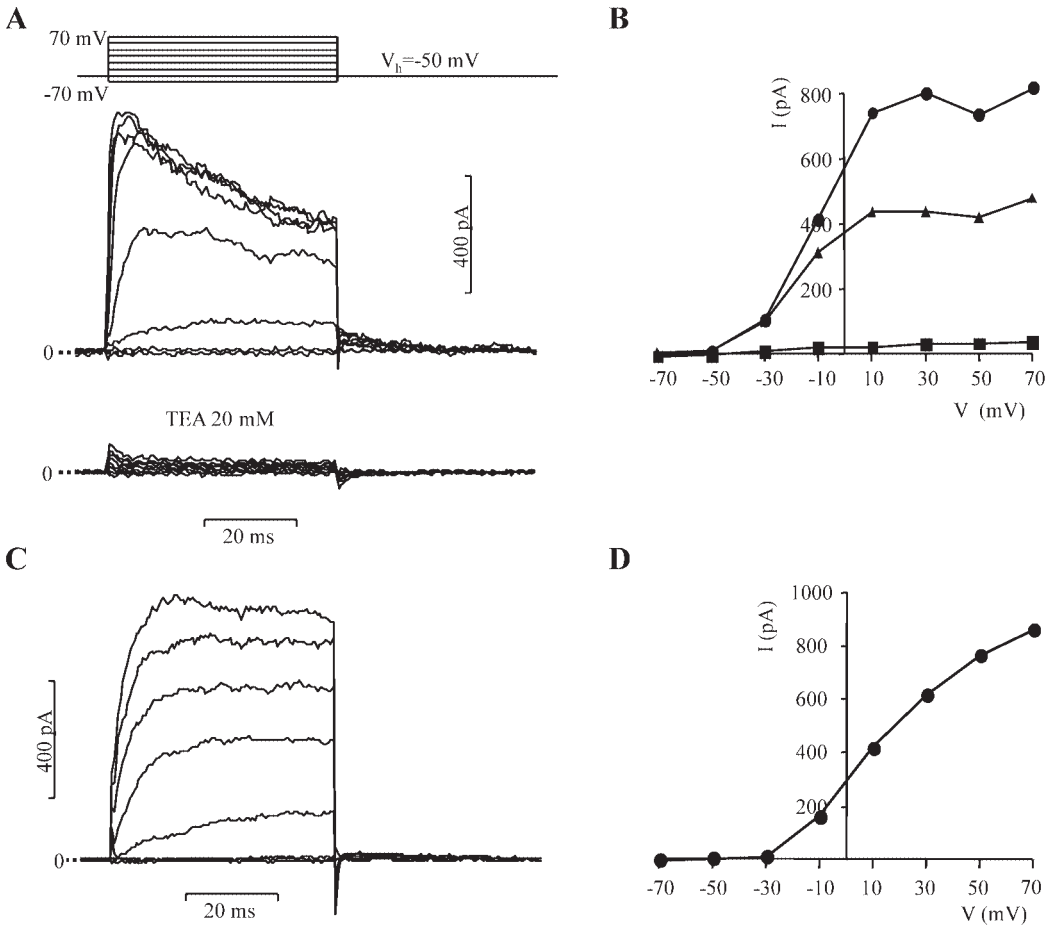

Figure 4 Outward K+ currents from isolated mouse olfactory sensory neurons. **(A)** Total outward currents evoked by 50 ms voltage-steps from –70 to +70 mV from a holding potential of –50 mV, according to the voltage protocol shown in the upper trace. The lower panel shows that bath application of 20 mM TEA on the same cell strongly reduced the outward currents suggesting that they are due to K^+ channels. Dotted lines indicate the zero current level. **(B)** Current–voltage relations from the recordings shown in (A) for the peak outward current (circles), the sustained current at the end of the voltage step (triangles) and the mean current measured in the presence of TEA (squares). **(C)** Outward currents from another olfactory sensory neuron activated by the same protocol as in (A). In this cell at a holding potential of –50 mV there was only a sustained component of the outward current. **(D)** Current–voltage relations from the recordings shown in (C).

hyperpolarization was necessary to remove inactivation of the I_A current.

Responses to odorants

The response of isolated mouse olfactory sensory neurons to odorants was studied by exposing cells for 1 s to a Ringer solution containing 0.5 mM of the odorant cineole. Figure 5A illustrates the inward current response of an isolated neuron to cineole in the whole-cell configuration voltage-clamped at –50 mV. We found that 12% of the cells (4 out of 32) responded to cineole with an inward current.

Olfactory sensory neurons were also exposed to IBMX, a well known phosphodiesterase inhibitor. Cells were exposed for 1 s to 1 mM IBMX and a responsive cell is illustrated in Figure 5B: the inward current response is presumably due to the increased concentration of cyclic AMP, and is similar to that induced by cineole (Figure 5A). Thirteen percent of the cells (6 out of 47) responded to IBMX with an inward current.

To our knowledge, these are the first recordings in the whole-cell configuration of odorant responses from isolated mouse olfactory sensory neurons. Previous reports have used the cell-attached patch-clamp (Maue and Dionne, 1987) or the suction pipette technique with isolated cells (Reisert and Matthews, 2001), or the perforated patch-clamp technique in the intact epithelium (Ma *et al.*, 1999; Ma and Shepherd, 2000) (see Discussion).

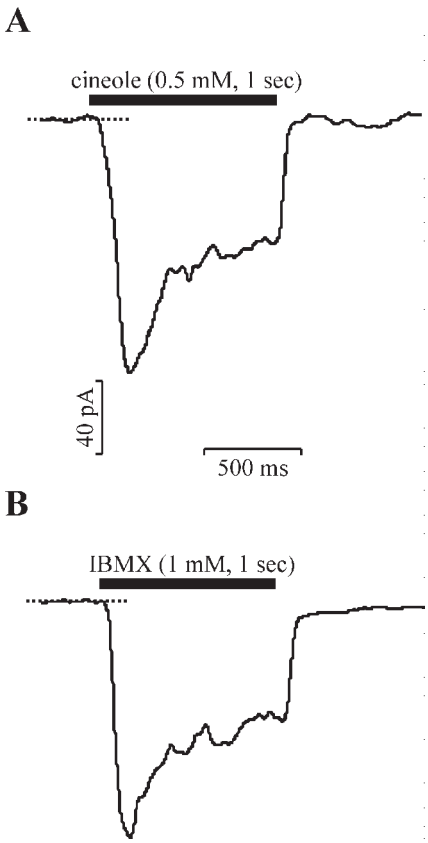

Figure 5 Whole-cell current responses of isolated mouse olfactory sensory neurons to odorant and to the phosphodiesterase inhibitor IBMX. Current responses were measured holding the voltage at –50 mV. The inward current was elicited by exposing a cell for 1 s to 0.5 mM cineole **(A)** or to 1 mM IBMX **(B)**. Recordings are from two different cells. The time course of the stimuli is shown at the top of each trace.

Responses to cyclic nucleotides

We first studied responses induced by intracellular cyclic nucleotides by introducing cyclic AMP into the cytoplasm of isolated olfactory sensory neurons by diffusion through the patch pipette. Figure 6A shows the result of an experiment in which 0.1 mM cAMP was added to the intracellular solution filling the patch pipette. Soon after the patch membrane was ruptured to obtain the whole-cell configuration cyclic AMP could freely diffuse into the olfactory sensory neuron. The introduction of cAMP into the cell produced an inward current that started after the rupture of the membrane

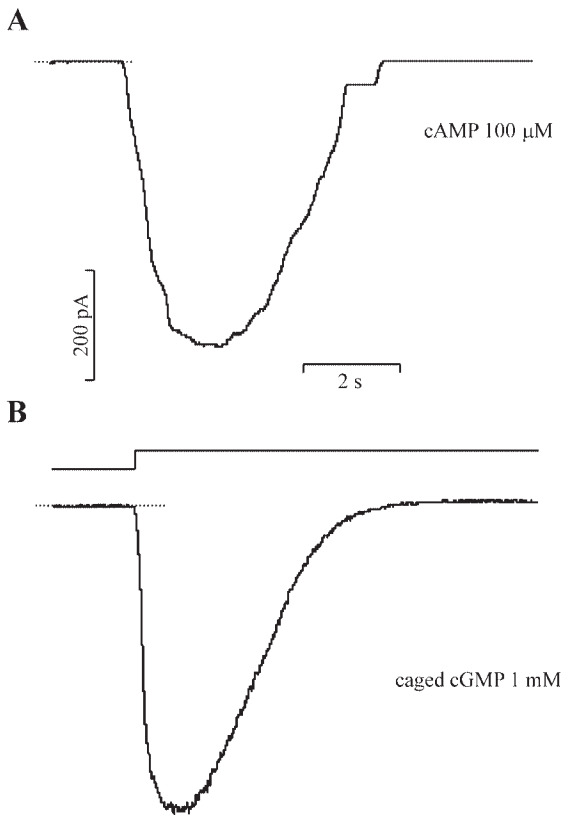

Figure 6 Transient inward currents induced in isolated mouse olfactory sensory neurons by continuous introduction of cyclic nucleotides. **(A)** The patch pipette contained 0.1 mM cAMP, that diffused into the cell after obtaining the whole-cell configuration. A transient inward current was activated by continuous diffusion of cAMP into the cell at the holding potential of –50 mV. **(B)** The patch pipette contained 1 mM caged cGMP, that diffused into the cell after obtaining the whole-cell configuration. The cell was illuminated by ultraviolet light from the time indicated at the top of the recording. A transient inward current was induced by the continuous photolysis of caged cGMP at the holding potential of –50 mV. Recordings are from two different cells.

patch, reached a peak in ~1–2 s and decayed back to baseline in 3–4 s. Therefore, the response was transient, even though cAMP was continuously supplied by diffusion from the patch pipette. These results are in agreement with previous detailed investigation on the response induced by intracellular cyclic nucleotides in olfactory sensory neurons isolated from amphibians (Kurahashi, 1990).

The introduction of compounds inside the cell by free diffusion from the patch pipette is a useful technique to measure activation or modification of channels, but it does not allow to change the concentration of the tested compounds or to perform control experiments in the same cell. A better way of studying the effect of various substances inside a cell is the use of caged compounds. Caged compounds are physiologically inert and flashes of ultraviolet light can be used to produce reproducible increases of the physiologically active compound inside the cell.

Cyclic nucleotides are available as caged compounds and have been used in olfactory sensory neurons in amphibians (Lowe and Gold, 1993a,b; Kurahashi and Menini, 1997; Takeuchi and Kurahashi, 2002) and in rats (Lowe and Gold, 1993b; Bradley *et al.*, 2001). We characterized the current induced by photolysis of caged cyclic nucleotides in olfactory sensory neurons from mice. Figure 6B illustrates the current induced by photolysis of 1 mM caged cGMP added to the intracellular solution in the patch pipette. When the membrane patch was ruptured to obtain the whole-cell configuration and caged cGMP diffused into the mouse olfactory sensory neuron from the patch pipette, it did not produce any measurable effect but, when an ultraviolet flash was applied to the entire cell to release the physiologically active cGMP, an inward current was induced. In this experiment, caged cGMP was continuously diffusing from the patch pipette into the cell and a long flash of 20 s was applied to the entire cell to cause a continuous photolysis of cGMP. This experiment is similar to that illustrated in Figure 6A where cAMP was continuously diffusing into the cell. A comparison between the two traces shows that the current increased and decayed to baseline with similar kinetics. Another ultraviolet flash after ~60 s was able to elicit a current (data not shown).

We found that 94% of the cells (44 out of 47) responded with an inward current to photolysis of caged cyclic nucleotides. Taking advantage of the reversibility and reproducibility of experiments with caged cyclic nucleotides, we investigated how changing the cyclic nucleotide concentration in the same cell affects the amplitude and time course of the induced current. Cyclic nucleotide concentration is entirely controlled by the intensity and duration of the ultraviolet flash. In a first set of experiments 1 mM caged cGMP was added to the patch pipette and various amounts of cGMP were photo-released by varying the duration of the ultraviolet flash illuminating the entire cell and maintaining the light intensity constant. This type of experiment is shown in Figure 7, in which the responses of an olfactory sensory neuron to brief flashes of different durations were plotted superimposed. The interval between flashes was at least 60 s. Currents rose immediately after the beginning of the flash, reached a peak after ~2 s and fell with a slow time course, decaying back to baseline over a time course of a few seconds.

To quantify the response of the cell to various durations of the flash, we constructed the dose-response relationship. Peak currents were normalized to the maximal value and plotted versus the flash duration. Data were well fitted by the Hill equation

$$I/I_{max} = t^n/(t^n + K_{1/2}{}^n)$$

where t is the flash duration, $K_{1/2}$ is the flash duration producing half of the maximal current and n is the Hill coef-

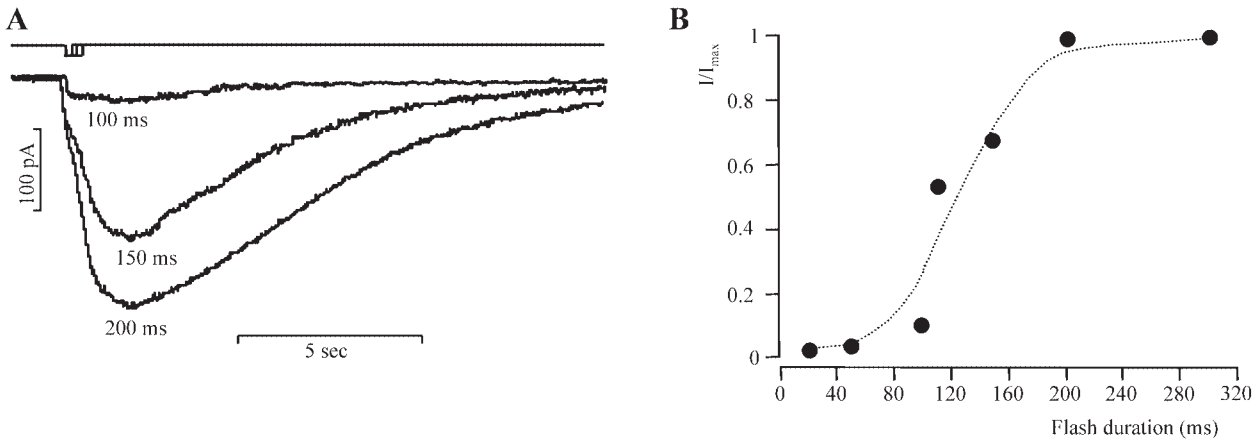

Figure 7 Whole-cell current responses induced in isolated mouse olfactory sensory neurons by photolysis of caged cyclic nucleotides as a function of flash duration. **(A)** 1 mM caged cGMP diffused into the cell from the patch pipette and flashes of increasing duration were applied to the cell eliciting inward currents of increasing amplitude. The holding potential was –50 mV. **(B)** Normalized peak currents from the cell in (A) were plotted versus flash duration. Data were fitted by the Hill equation $I/I_{max} = t^n/(t^n + K_{1/2}{}^n)$ with $K_{1/2}$ = 122 ms and n = 5.3.

ficient. The best fit gave $K_{1/2}$ = 122 ms and n = 5.3. Similar values were obtained from two other cells and are consistent with previous results in amphibian olfactory sensory neurons (Kurahashi and Menini, 1997; Takeuchi and Kurahashi, 2002).

To investigate the kinetics of the current induced by photolysis of cyclic nucleotides we performed a second set of experiments measuring currents elicited by uncaging cyclic nucleotides from various localized regions of the olfactory sensory neuron. In fact, in the previously described experiments, the entire cell was illuminated by a flash and, therefore, cGMP was uncaged everywhere in the cell cytoplasm. By using a flash-lamp system with a light-guide (see Methods section) we were able to obtain a light spot to illuminate selected regions of the cell. The flash-lamp system we used allows the delivery of very short flashes (0.6 ms) of high intensity. Figure 8A shows currents induced by producing local photolysis in the ciliary region (left) or in the cell body (right) in two different cells. Currents were normalized to their peak values and plotted superimposed in Figure 8B,C. The rising phase of the response was faster and the latency was shorter when the flash was localized to the cilia compared with the cell body. The latency was 5–10 ms for flashes on the cilia and 200–400 ms for flashes on the cell body. The rising phase from several olfactory sensory neurons in the two experimental conditions were fitted by an

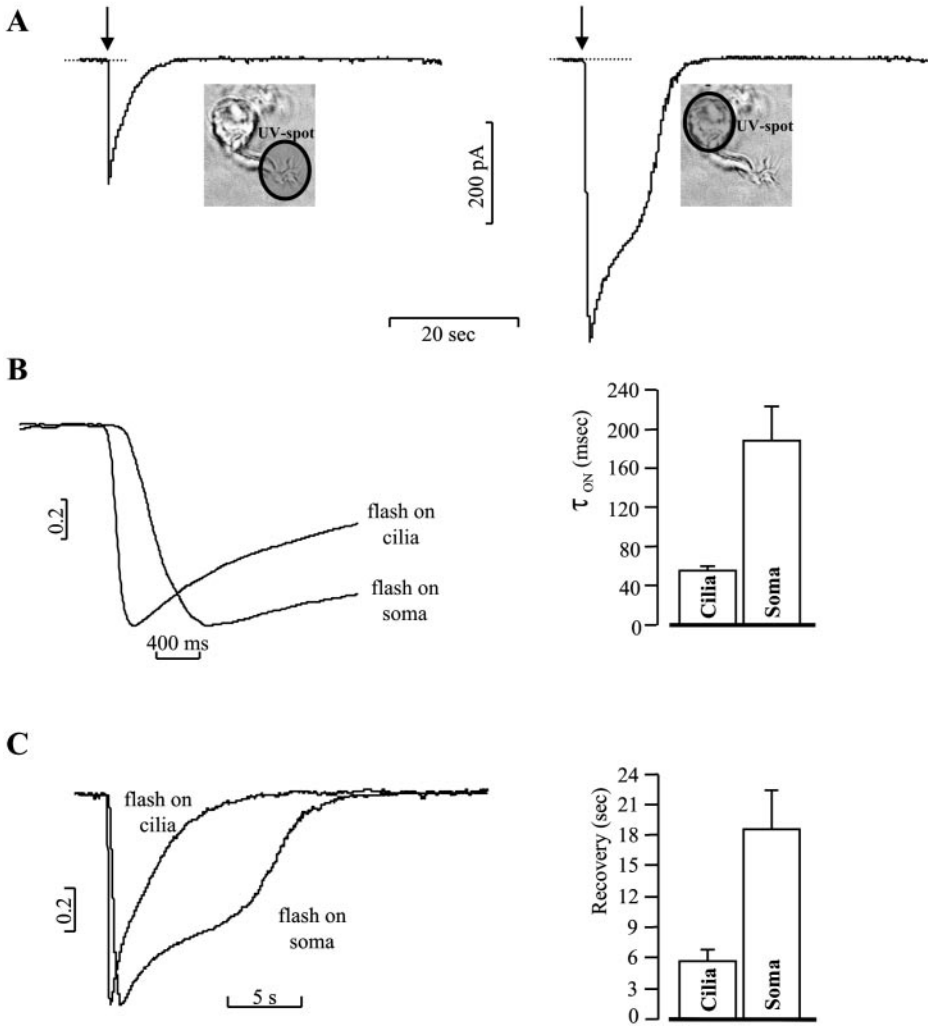

Figure 8 Whole-cell current responses induced in isolated mouse olfactory sensory neurons by photolysis of caged cyclic nucleotides localized to the cilia or to the soma. A flash lamp with an optical fiber was used to deliver short flashes (0.6 ms) to localized regions of the cell. **(A)** Currents elicited by photolysis in the cilia (left) or in the cell body (right) from two different cells. The timing of the light flash is indicated by the arrow. The holding potential was –50 mV. **(B)** On the left normalized currents are superimposed on an expanded time scale to show the differences in the latency and the rising phase of the responses. The rising phase from individual experiments was fitted by an exponential function and the mean values of the time constants are plotted on the right: 55 ± 4 ms (n = 7) for photolysis in the cilia and 187 ± 34 ms (n = 11) for photolysis in the cell body. **(C)** On the left, normalized currents are superimposed to show the difference in time for recovery of the current from the peak to baseline. Mean values of the recovery time are plotted on the right: 5.6 ± 0.9 s (n = 7) for flashes on the cilia and 18.7 ± 3.7 s (n = 11) for flashes on the soma.

exponential curve, and the mean values of the time constants were 55 ± 4 ms (n = 7) for photolysis in the cilia and 187 ± 34 ms (n = 11) for photolysis in the cell body (see right panel in Figure 8B). Also the recovery of the induced current to baseline was different, being faster when the flash was localized to the cilia compared to the cell body. The time for recovery of current to baseline was measured as the time interval between the peak current and the return to baseline. Mean values were 5.6 ± 0.9 s (n = 7) for flashes on the cilia and 18.7 ± 3.7 s (n = 11) for flashes on the soma (see right panel in Figure 8C).

These results indicate that latency, rising time and recovery to baseline of the cyclic nucleotide-induced response are strongly dependent on the site of photolysis and are consistent with previous experiments obtained in olfactory sensory neurons from the salamander (Lowe and Gold, 1993a).

Finally, the dependence of the photolysis-induced current on light intensity was investigated. Currents were measured with the flash-lamp system as the light intensity was varied, while the flash duration was constant at 0.6 ms. Peak currents were normalized to the maximal value and plotted as a function of the relative light intensity in Figure 9. Data were fitted by the Hill equation

$$I/I_{max} = i^n/(i^n + K_{1/2}{}^n)$$

where i is the relative light intensity, $K_{1/2}$ is the half-maximal relative intensity and n is the Hill coefficient. The best fit gave $K_{1/2}$ = 0.35 and n = 3.2. Similar results were obtained from two other cells.

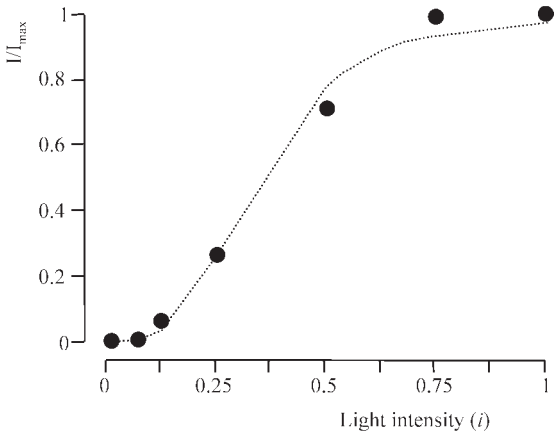

Figure 9 Whole-cell current responses induced in isolated mouse olfactory sensory neurons by photolysis of caged cyclic nucleotides as a function of light intensity. 1 mM caged cGMP diffused into the cell from the patch pipette and flashes of increasing intensity were applied to the cilia at the holding potential of –50 mV. The peaks of the light-induced current responses were normalized to the maximal value and plotted versus the relative light intensity. Data were fitted by the Hill equation $I/I_{max} = i^n/(i^n + K_{1/2}{}^n)$ with $K_{1/2}$ = 0.35 and n = 3.3.

Discussion

Resting potential and voltage-gated currents

We have measured resting membrane potentials in olfactory sensory neurons isolated from the mouse ranging from –45 to –90 mV, with a mean value of –55.4 ± 3.6 mV (n = 237) and these values are in general agreement with those measured by other groups in mouse olfactory sensory neurons. Maue and Dionne (1987) using the cell-attached technique estimated a membrane potential in the range of –30 to –80 mV, with a mean of –52 ± 17 mV (n = 10), Ma *et al.* (1999) using the perforated patch technique found a mean value of –55 ± 3.5 mV (n = 19) (Liman and Corey, 1996) in the whole-cell configuration obtained a mean of –81.8 ± 2.1 mV (n = 6). In the rat, the resting membrane potential measured by Lynch and Barry (1991) was in the range –40 to –73 mV, with a mean of –52 ± 4 mV (n = 9), while in amphibians measurements of the resting membrane potential in the whole-cell configuration gave values ranging from –30 to –72 mV (Trotier, 1986; Firestein and Werblin, 1987; Schild, 1989; Kawai *et al.*, 1996).

However, these measured membrane resting potentials are likely to be underestimated, as previously discussed in detail (Lynch and Barry, 1989, 1991; Schild, 1989; Schild and Restrepo, 1998). In fact, to have a reliable measurement of the membrane resting potential, it is necessary that the resistance of the seal between the patch pipette and the cell membrane is much higher than the resistance of the cell membrane. However, olfactory sensory neurons from the various species have a very high membrane resistance (between 1 to 40 GΩ) that, in mouse olfactory sensory neurons, was estimated to be 2.9 ± 0.8 GΩ (n = 8) by Liman and Corey (1996) and 4.1 ± 0.6 GΩ (n = 6) by Ma *et al.* (1999). Since seal resistances are usually a few GΩ (with occasional higher values up to 50 GΩ), and therefore, are similar to the membrane resistance, in most recordings the measured membrane resting potential is underestimated and the real resting potential is more negative than the measured one (for a detailed description, see Schild and Restrepo, 1998, pp. 432–433). As a result, it is likely that the mean value does not have a physiological relevance and that the real resting potential is near the more negative measured value. Therefore, from our recordings, it is likely that the real resting potential is closer to the more negative values between –70 and –90 mV rather than to the total mean value of –55.4 mV.

That the real resting potential of mouse olfactory sensory neurons is more negative than –55 mV would also be consistent with the activation and inactivation properties we measured for the Na^+ currents, that are responsible for spike initiation after generation of the receptor potential caused by the odorant-induced current. In fact, we showed that, when the holding potential was between –90 and –70 mV, we measured inward currents of decreasing amplitude (see Figure 2) and, when the holding potential was –50 mV we

did not record any inward current (see Figure 4). This is consistent with the inactivation curves we have measured for Na^+ channels (Figure 3), showing that there is a substantial inactivation of the Na^+ current at membrane potentials more positive than –60 mV and therefore that not many Na^+ channels would be available for generation of action potential. These results are also consistent with the Na^+ channel properties measured by Ma *et al.* (1999) in the mouse intact epithelial preparation. A comparison with other species of the Na^+ half-inactivation voltage shows that the value obtained in our studies for mouse olfactory sensory neurons, –75 mV, is comparable to that in the catfish, –78 mV (Corotto *et al.*, 1996), but is more positive than that measured in the rat, –108 mV (Rajendra *et al.*, 1992; Qu *et al.*, 2000), and more negative than that measured in amphibians: –50 mV in the larval tiger salamander (Firestein and Werblin, 1987) and –53 mV in the newt (Kawai *et al.*, 1996). These differences could be due to interspecies variability or to the different experimental protocols used in different laboratories.

The repolarization of action potentials is due to the activation of K^+ channels. We have described the presence of at least two outward K^+ currents distinguishable by their kinetics: a rapidly inactivating, I_A, and a delayed rectifier, I_K, component (Figure 4). In some cells the I_A component could be activated by depolarization from a holding potential of –50 mV, while in others it was inactivated, but the steady-state inactivation could be removed by hyperpolarizing the cell to –80 mV (data not shown). Therefore, in our experiments both I_A and I_K components appeared to be present in most mouse olfactory sensory neurons, similarly to the results in the mouse intact epithelial preparation (Ma *et al.*, 1999). A comparison with the K^+ currents in olfactory sensory neurons of other species shows that both the I_A and the I_K component were found in amphibians (Trotier, 1986; Firestein and Werblin, 1987; Schild, 1989), while in rats the delayed rectifier was frequently absent (Lynch and Barry, 1991). Therefore, the measured inward and outward currents play similar roles in spike generation and repolarization with minor differences among various species.

Odorant-induced responses

We showed that it is possible to record responses to odorants from olfactory sensory neurons isolated from the mouse in the whole-cell voltage-clamp configuration and that such responses were mimicked by the phosphodiesterase inhibitor IBMX (Figure 5). We found that only 13% of cells, responded with a measurable inward current to application of IBMX. Previous measurements by Ma *et al.* (1999) obtained using the perforated patch-clamp technique in individual cells in the intact olfactory epithelium, reported that a higher percentage of cells (55%) responded to IBMX. Although it could be suggested that the lower percentage of responses to IBMX in our experiments is caused by the loss of some intracellular component by the use of the whole-cell versus the perforated-patch configuration, our results are consistent with those of Bozza *et al.* (2002) obtained in intact cells. Bozza *et al.* (2002) applied calcium imaging to characterize the odorant response properties of isolated olfactory sensory neurons from the mouse and found that brief pulses of 500 μM IBMX did not consistently induce somatic calcium changes, while 10 μM forskolin always elicited a calcium response in odorant-responsive olfactory sensory neurons. Since IBMX causes an increase in the intracellular cAMP concentration by inhibiting PDE, without affecting the basal adenylyl cyclase activity, while forskolin is an activator of cyclase activity, we suggest that cells not responding to IBMX had a very low basal cyclase activity.

Investigating the responses to the odorant cineole, we found that 12% of the tested mouse olfactory sensory neurons responded with an inward current. These results are similar to a previous study in amphibians in which odorant responses from the salamander were investigated in the same experimental conditions, and it was found that 22% olfactory sensory neurons responded to cineole with an inward current (Firestein *et al.*, 1993; Menini *et al.*, 1995). Our results were further compared with other published work. To our knowledge, there are only two published reports (Maue and Dionne, 1987; Reisert and Matthews, 2001) in which isolated olfactory sensory neurons dissociated from the mouse olfactory epithelium were tested for their responses to odorants. Two other studies investigated odorant responses from individual neurons in the intact mouse olfactory epithelium (Ma *et al.*, 1999; Ma and Shepherd, 2000). Maue and Dionne (1987) applied a mixture of odorants to isolated cells and recorded in the cell-attached configuration an increase in membrane conductance in 25% of the cells, but did not record in the whole-cell configuration. Reisert and Matthews (2001) used the suction pipette technique and measured inward currents in cells stimulated with the odorant cineole by using a similar perfusion system to the one that we used, but did not report the percentage of odorant responsive cells. Ma *et al.* (1999) and Ma and Shepherd (2000) recorded responses to a mixture of four odorants, including cineole, from individual olfactory sensory neurons in the mouse intact epithelium with the perforated patch-clamp technique and found that 28% of the cells responded with an inward current.

Together, these results indicate that the inward responses to odorants are similar in the salamander and in the mouse.

Photolysis of caged compounds

In the present study, photolysis of caged cyclic nucleotides produced an inward current in 94% of mouse olfactory sensory neurons. The time course of the response differed considerably depending on the site of cyclic nucleotide photolysis. When cyclic nucleotides were photolyzed in the cilia, the response had a short latency and rapid rising time, when photolyzed in the cell body, the latency was longer and the rising time slower. The longer latency and rising time of

the response when cyclic nucleotides were photolyzed far from the cilia can be accounted for by the time needed for diffusion of the cyclic nucleotide, that can be calculated by using the relation $r^2 = 2Dt$ (Hille, 2001, p. 313), where r^2 is the mean-square displacement in one dimension of the diffusing molecule, D is the diffusion coefficient and t is the time. The diffusion coefficient of cAMP in frog olfactory cilia has been estimated by (Chen *et al.*, 1999; Qu *et al.*, 2000) to be 2.7×10^{-6} cm^2/s and therefore the time needed for cAMP to cover a distance of 10 μm is 185 ms, while for 20 μm it is 740 ms. These values are in general agreement with the measured response latency of 200–400 ms, and the mean time constant for the rising time of 187 ms when cyclic nucleotides were photolyzed into the cell body.

We also found that the time for recovery of photolysis responses elicited by illuminating the soma was longer (18.7 s) than that measured when only the cilia were illuminated (5.6 s). Since cyclic nucleotides are hydrolyzed by PDE that is mainly localized in the cilia (Borisy *et al.*, 1992), the difference in the duration of the response is probably caused by the large reservoir of cyclic nucleotides that are not hydrolyzed in the soma.

These experiments not only confirm previous reports in amphibians on the localization of cyclic nucleotide gated channels to the cilia (Lowe and Gold, 1993a) but also point out the importance of the careful localization of photolysis when experiments are done to infer kinetics parameters from comparing the effect of photolysis of caged compounds with odorant-induced currents, since diffusion of cyclic nucleotides could modify the measured kinetics.

The relation between membrane current and light intensity was nonlinear and was fitted by a Hill equation with a cooperativity 3.2. As previously pointed out, this value of cooperativity resides primarily in current generation, and not in cyclic nucleotide metabolism, since changes in cyclic nucleotide concentrations were produced directly by flash photolysis without activating the transduction pathway (Lowe and Gold, 1993b; Kurahashi and Menini, 1997; Takeuchi and Kurahashi, 2002). Moreover, it has been shown that the inward current activated by photolysis of cyclic nucleotides is carried not only through the channels gated by cyclic nucleotides, but also by a current through chloride channels activated by Ca^{2+} entering through the cyclic nucleotide activated channels (Lowe and Gold, 1993b). We have found that also in mouse olfactory sensory neurons a fraction of the total current activated by cyclic nucleotides could be blocked by SITS, an inhibitor of Ca^{2+}-activated chloride channels (data not shown). Therefore, also in mouse olfactory sensory neurons the cooperativity value measured in Figure 9 arises by the nonlinear contribution to the total current of both cyclic nucleotide-gated channels and Ca^{2+}-activated Cl^- channels.

Together these results demonstrate that, although technically difficult, it is possible to record in the whole-cell configuration from olfactory sensory neurons isolated from the mouse. Odorant-induced currents can be recorded and caged compounds can be introduced into the cytoplasm via the patch pipette and photolyzed. This approach could be used in the future to investigate the responses of olfactory sensory neurons from mice carrying genetic modifications to unravel further aspects of the olfactory transduction cascade.

Acknowledgements

We thank Dylan Dean and Andrea Mazzatenta for technical and scientific suggestions, Anna Boccaccio for comments on the manuscript, and Manuela Schipizza-Lough for secretarial assistance. This work was supported by grants from NATO, the Italian Minister of University and Scientific Research, and the European Union.

References

Borisy, F.F., Ronnett, G.V., Cunningham, A.M., Juilfs, D., Beavo, J. and **Snyder, S.H.** (1992) *Calcium/calmodulin-activated phosphodiesterase expressed in olfactory receptor neurons*. J. Neurosci., 12, 915–923.

Bozza, T.C. and **Kauer, J.S.** (1998) *Odorant response properties of convergent olfactory receptor neurons*. J. Neurosci., 18, 4560–4569.

Bozza, T., Feinstein, P., Zheng, C. and **Mombaerts, P.** (2002) *Odorant receptor expression defines functional units in the mouse olfactory system*. J. Neurosci., 22, 3033–3043.

Bradley, J., Reuter, D. and **Frings, S.** (2001) *Facilitation of calmodulin-mediated odor adaptation by cAMP-gated channel subunits*. Science, 294, 2176–2178.

Breer, H. (2003) *Sense of smell: recognition and transduction of olfactory signals*. Biochem. Soc. Trans., 31, 113–116.

Buck, L.B. (2000) *The molecular architecture of odor and pheromone sensing in mammals*. Cell, 100, 611–618.

Chen, C., Nakamura, T. and **Koutalos, Y.** (1999) *Cyclic AMP diffusion coefficient in frog olfactory cilia*. Biophys. J., 76, 2861–2867.

Corotto, F.S., Piper, D.R., Chen, N. and **Michel, W.C.** (1996) *Voltage- and Ca(2+)-gated currents in zebrafish olfactory receptor neurons*. J. Exp. Biol., 199, 1115–1126.

Firestein, S. (2001) *How the olfactory system makes sense of scents*. Nature, 413, 211–218.

Firestein, S. and **Werblin, F.S.** (1987) *Gated currents in isolated olfactory receptor neurons of the larval tiger salamander*. Proc. Natl Acad. Sci. USA, 84, 6292–6296.

Firestein, S., Picco, C. and **Menini, A.** (1993) *The relation between stimulus and response in olfactory receptor cells of the tiger salamander*. J. Physiol., 468, 1–10.

Frings, S., Seifert, R., Godde, M. and **Kaupp, U.B.** (1995) *Profoundly different calcium permeation and blockage determine the specific function of distinct cyclic nucleotide-gated channels*. Neuron, 15, 169–179.

Frings, S., Reuter, D. and **Kleene, S.J.** (2000) *Neuronal Ca2+ -activated Cl- channels–homing in on an elusive channel species*. Prog. Neurobiol., 60, 247–289.

Gavazzo, P., Picco, C., Eismann, E., Kaupp, U.B. and **Menini, A.** (2000) *A point mutation in the pore region alters gating, Ca(2+) blockage, and permeation of olfactory cyclic nucleotide-gated channels*. J. Gen. Physiol., 116, 311–326.

Hille B. (2001) Ion Channels of Excitable Membranes, 3rd edn. Sinauer, Sunderland, MA.

Kawai, F., Kurahashi, T. and **Kaneko, A.** (1996) *T-type Ca2+ channel lowers the threshold of spike generation in the newt olfactory receptor cell*. J. Gen. Physiol., 108, 525–535.

Kleene, S.J. (1993) *Origin of the chloride current in olfactory transduction*. Neuron, 11, 123–132.

Kleene, S.J. and **Gesteland, R.C.** (1991) *Calcium-activated chloride conductance in frog olfactory cilia*. J. Neurosci., 11, 3624–3629.

Kurahashi, T. (1990) *The response induced by intracellular cyclic AMP in isolated olfactory receptor cells of the newt*. J. Physiol., 430, 355–371.

Kurahashi, T. and **Yau, K.W.** (1993) *Co-existence of cationic and chloride components in odorant-induced current of vertebrate olfactory receptor cells*. Nature, 363, 71–74.

Kurahashi, T. and **Menini, A.** (1997) *Mechanism of odorant adaptation in the olfactory receptor cell*. Nature, 385, 725–729.

Leinders-Zufall, T., Rand, M.N., Shepherd, G.M., Greer, C.A. and **Zufall, F.** (1997) *Calcium entry through cyclic nucleotide-gated channels in individual cilia of olfactory receptor cells: spatiotemporal dynamics*. J. Neurosci., 17, 4136–4148.

Leinders-Zufall, T., Greer, C.A., Shepherd, G.M. and **Zufall, F.** (1998) *Visualizing odor detection in olfactory cilia by calcium imaging*. Ann. N. Y. Acad. Sci., 855, 205–207.

Liman, E.R. and **Corey, D.P.** (1996) *Electrophysiological characterization of chemosensory neurons from the mouse vomeronasal organ*. J. Neurosci., 16, 4625–4637.

Lowe, G. and **Gold, G.H.** (1993a) *Contribution of the ciliary cyclic nucleotide-gated conductance to olfactory transduction in the salamander*. J. Physiol., 462, 175–196.

Lowe, G. and **Gold, G.H.** (1993b) *Nonlinear amplification by calcium-dependent chloride channels in olfactory receptor cells*. Nature, 366, 283–286.

Lynch, J.W. and **Barry, P.H.** (1989) *Action potentials initiated by single channels opening in a small neuron (rat olfactory receptor)*. Biophys. J., 55, 755–768.

Lynch, J.W. and **Barry, P.H.** (1991) *Properties of transient K+ currents and underlying single K+ channels in rat olfactory receptor neurons*. J. Gen. Physiol., 97, 1043–1072.

Ma, M. and **Shepherd, G.M.** (2000) *Functional mosaic organization of mouse olfactory receptor neurons*. Proc. Natl Acad. Sci. USA, 97, 12869–12874.

Ma, M., Chen, W.R. and **Shepherd, G.M.** (1999) *Electrophysiological characterization of rat and mouse olfactory receptor neurons from an intact epithelial preparation*. J. Neurosci. Methods, 92, 31–40.

Maue, R.A. and **Dionne, V.E.** (1987) *Patch-clamp studies of isolated mouse olfactory receptor neurons*. J. Gen. Physiol., 90, 95–125.

Menini, A. (1999) *Calcium signalling and regulation in olfactory neurons*. Curr. Opin. Neurobiol., 9, 419–426.

Menini, A., Picco, C. and **Firestein, S.** (1995) *Quantal-like current fluctuations induced by odorants in olfactory receptor cells*. Nature, 373, 435–437.

Mombaerts, P. (1999) *Molecular biology of odorant receptors in vertebrates*. Annu. Rev. Neurosci., 22, 487–509.

Nakamura, T. and **Gold, G.H.** (1987) *A cyclic nucleotide-gated conductance in olfactory receptor cilia*. Nature, 325, 442–444.

Qu, W., Moorhouse, A.J., Rajendra, S. and **Barry, P.H.** (2000) *Very negative potential for half-inactivation of, and effects of anions on, voltage-dependent sodium currents in acutely isolated rat olfactory receptor neurons*. J. Membr. Biol., 175, 123–138.

Rajendra, S., Lynch, J.W. and **Barry, P.H.** (1992) *An analysis of Na+ currents in rat olfactory receptor neurons*. Pflugers Arch., 420, 342–346.

Reisert, J. and **Matthews, H.R.** (2001) *Response properties of isolated mouse olfactory receptor cells*. J. Physiol., 530, 113–122.

Restrepo, D., Miyamoto, T., Bryant, B.P. and **Teeter, J.H.** (1990) *Odor stimuli trigger influx of calcium into olfactory neurons of the channel catfish*. Science, 249, 1166–1168.

Schild, D. (1989) *Whole-cell currents in olfactory receptor cells of* Xenopus laevis. Exp. Brain Res., 78, 223–232.

Schild, D. and **Restrepo, D.** (1998) *Transduction mechanisms in vertebrate olfactory receptor cells*. Physiol Rev., 78, 429–466.

Spehr, M., Wetzel, C.H., Hatt, H. and **Ache, B.W.** (2002) *3-Phosphoinositides modulate cyclic nucleotide signaling in olfactory receptor neurons*. Neuron, 33, 731–739.

Takeuchi, H. and **Kurahashi, T.** (2002) *Photolysis of caged cyclic AMP in the ciliary cytoplasm of the newt olfactory receptor cell*. J. Physiol., 541, 825–833.

Trotier, D. (1986) *A patch-clamp analysis of membrane currents in salamander olfactory receptor cells*. Pflugers Arch., 407, 589–595.

Zhainazarov, A.B. and **Ache, B.W.** (1995) *Odor-induced currents in Xenopus olfactory receptor cells measured with perforated-patch recording*. J. Neurophysiol., 74, 479–483.

Accepted September 2, 2003